# Forecasting of a Large Earthquake: An Outlook of the Research

by Yosihiko Ogata

## ABSTRACT

Although the unconditional probability of a major earthquake in an area is extremely small, the probability can increase in the presence of anomalies that act as potential precursors. Precursor-like anomalies of only a single type may not sufficiently enhance the probability of a large earthquake, but the probability can be substantially increased using the multielements prediction formula when independent precursor-like anomalies of plural types are observed at the same time. Despite some illustrative applications for successful predictions in the late 1970s, this idea has seldom been applied for more than 40 yrs. This is because of the scarcity of remarkable anomalies preceding large earthquakes and a lack of extensive statistical studies on anomalies relative to large earthquakes, which prevents stable assessment estimates of probability gains. This article aims to provide an outlook for future study on these issues. I focus on evaluating the probability gains of a large earthquake using anomalies of seismic activity based on statistical diagnostic analysis. Specifically, I illustrate the evaluation methods with reference to seismic activity before the 2016 **M** 7.3 Kumamoto earthquakes. Furthermore, I discuss outlooks using similar and extended approaches in seismicity and other monitoring fields.

## INTRODUCTION

Although the unconditional probability of a major earthquake in a specific area is very small, the probability may increase when information about anomalies that act as potential precursors and other relevant information is available. Specifically, we can estimate the conditional probability of a major earthquake occurring in the presence of observed anomalies and other information, and also increase the probability gain; that is, the ratio of the conditional probability to the underlying unconditional probability. This compels us to perform quantitative studies on the statistics of anomalies against earthquakes using relevant data sets such as the causal relations of anomalies and other predictive factors relative to major earthquakes.

Furthermore, abnormal phenomena of only a single type may not sufficiently enhance the ordinary probability of an earthquake. However, observing independent abnormal phenomena of plural types during the relevant period can further increase the probability. Using observations of long-term, medium-term, and short-term anomalies, we should look for knowledge and abnormal phenomena that can constitute the multielements prediction formula of Utsu (1977). Aki (1981) confirmed the formula using the Bayes rule, which assumes that precursory anomalies are mutually independent of each other, and then approximated the multielements formula by the multiplication of probability gains (see Appendix). In the Plural Precursory Anomaly Phenomena section, I summarize the retrospective forecasting procedure used in the case of the 1978 **M** 7.0 Izu Kinkai earthquake calculated by Utsu (1979a).

However, as far as I am aware, a multielements prediction formula has not been implemented for more than 40 yrs despite its importance. One reason for this is the scarcity of clearly recognizable anomalies preceding large earthquakes, which has prevented stable estimates of probability gains. Furthermore, we have not completed sufficient statistical studies on precursory anomalies for assessing the probability gains of large earthquakes despite the accumulation of large amounts of relevant data by various monitoring measurements.

This article considers seismicity anomalies such as relative quiescence in aftershock activity and statistical discrimination of foreshocks from other types of earthquake clusters, as well as the evaluation of active fault ruptures. We can obtain such anomalies and probability gains using statistical models of earthquake occurrence data and their diagnostic analysis. As an illustrative application, I retrospectively forecast an $\mathbf{M} \geq 7$ earthquake during the period preceding the 2016 **M** 7.3 Kumamoto earthquake in Kyushu, Japan. Furthermore, I discuss a possible outlook on relevant studies in seismic activity and other monitoring fields.

## PLURAL PRECURSORY ANOMALY PHENOMENA

In the second half of the 1970s, there were several anomalies observed in and around the Izu Peninsula, Japan, such as crustal uplift (gravity changes), volumetric anomalies, water level changes, and chemical radon component changes. Those anomalies were reported and discussed in the Coordinating Committee of Earthquake Prediction (CCEP, 1976–1978). Then, when seismic activity started near Izu-Oshima Island, the Japan Meteorological Agency (JMA) announced a warning a few hours before the 1978 **M** 7.0 Izu-Oshima-Kinkai earthquake occurred.

Later, Utsu (1979a) reviewed these anomalous events, and, based on his expert knowledge and opinion of past sequences in the Izu area, assigned the secular and conditional probabilities of occurrence of a target earthquake of $\mathbf{M} \geq 6.5$ based on

doi: 10.1785/0220170006

**Table 1**
**Multielement Prediction of Izu-Ohshima-Kinkai Earthquake**

| | 3 hours | 1 day | 3 days |
|---|---|---|---|
| Case I | | | |
| $P(\mathbf{M} \geq 6.5 \mid A \cap B \cap C)$ | 0.080 (0.011) | 0.41 (0.081) | 0.68 (0.21) |
| $P(\mathbf{M} \geq 6.5 \mid A \cap B)$ | 0.0024 | 0.019 | 0.056 |
| $P(\mathbf{M} \geq 6.5 \mid B \cap C)$ | 0.042 | 0.26 | 0.52 |
| Case II | | | |
| $P(\mathbf{M} \geq 6.5 \mid A \cap B \cap C)$ | 0.49 (0.11) | 0.89 (0.49) | 0.96 (0.75) |
| $P(\mathbf{M} \geq 6.5 \mid A \cap B)$ | 0.0079 | 0.060 | 0.16 |
| $P(\mathbf{M} \geq 6.5 \mid B \cap C)$ | 0.13 | 0.54 | 0.78 |

Probability of earthquake calculated using the multielement prediction formula (Utsu, 1979a). Conditional probabilities are given for three prediction intervals. In parentheses, probabilities are provided for cases when $P_A$, $P_B$, and $P_C$ (see text below for each of the probabilities) are each 1/2 of their original value or when $P_A \times P_B \times P_C$ is 1/8 of the original value, in the table. Cases I and II stand for the wider and narrower Izu region, respectively, where secular probability of the target earthquake is assumed.

long-term, medium-term, and short-term anomalies. Aki (1981) explained the bases of the Utsu's assessments as follows:

- (S) Secular probability of an **M** ≥ 6.5 earthquake (case I) for the wider Izu region is evaluated to be once per 30 yrs (e.g., $P_S = 0.009\%$ per day); (case II) for the narrower Izu region, the probability is evaluated to be once per 100 yrs ($P_S = 0.003\%$ per day).
- (A) As a long-term anomaly, uplift of Izu Peninsula took place, thus the earthquake probability is evaluated as 1/3 within 5 yrs ($P_A = 0.02\%$ per day) from when the uplift started.
- (B) The medium-term probability of an earthquake occurring within one month is 1/10 ($P_B = 0.3\%$ per day) based on the composite of radon anomalies, anomalous water table changes, and volumetric strain anomalies.
- (C) The short-term anomaly is that seismic activity started west of Oshima Island on the morning of 14 January. The foreshock probability is 1/35 within 3 days ($P_C = 1\%$ per day).

Because the three anomaly period scales for A, B, and C are markedly different in the time scale of appearance, Utsu (1977) regarded them as independent phenomena (see Appendix). Thus, based on the multielements probability formula (see equation A1), Utsu (1979a) obtained Table 1. Surprisingly, despite the conditional probabilities $P_A$, $P_B$, and $P_C$ are very small values; $P(\mathbf{M} \geq 6.5 \mid A \cap B \cap C)$ becomes considerably large, bounded in the 8%–89% range per day as given in Table 1.

Using a similar procedure, Cao and Aki (1983) assessed the probabilities as being nearly 10% per day just before the 1975 **M** 7.3 Haicheng earthquake and three other major earthquakes in China.

In general, we should only examine the probability values for each item after accumulating observation data over many years; it is difficult to gather earthquake prediction data, except for seismic activity, within a short time frame. Monitoring in and around the Izu Peninsula region has been special and exceptional because it is a natural laboratory with both strong earthquakes and various monitoring stations. Another dense real-time monitoring system has been operating near the Tokai District since 1979 to watch for an expected **M** 8 class Tokai earthquake (JMA, 2016). However, there have been few strong earthquakes or clearly recognizable anomalies except for slow slips around the focal region.

The following case introduces a similar evaluation procedure, in which only seismic information that may be applicable to the regions of intensive seismic activity in and around Japan are used.

## CASE OF KUMAMOTO EARTHQUAKE

On 16 April 2016, an **M** 7.3 earthquake occurred on the Futagawa fault in Kumamoto Prefecture, Kyushu Island, Japan (for the general references, see Hashimoto *et al.*, 2016–2017). Twenty-eight hours prior to this event, an **M** 6.5 earthquake occurred, followed by what seemed to be aftershocks, including an **M** 6.4 aftershock (Fig. 1b). This aftershock sequence was actually the foreshock activity of the **M** 7.3 earthquake. Figure 2 delineates snapshots of the short-term probability forecast using the hierarchical space–time epidemic-type aftershock sequence (HIST-ETAS) model (Ogata, 2011a) that was submitted to the Collaboratory for the Study of Earthquake Predictability Japan Testing Center (Nanjo *et al.*, 2011).

Ogata *et al.* (1996) formulated foreshock-type activity when the largest earthquake in the beginning of a cluster is replaced by a much larger earthquake with a difference of 0.45 or more in magnitude. During the period of aftershock activity between the **M** 6.5 and 7.3 earthquakes, I want to retrospectively evaluate such a probability. Namely, I assume the size of the target earthquake is **M** 7.0 or larger. Also, there were several medium-term seismicity anomalies in addition to the long-term probability of large earthquakes in this region. In the following sections, I retrospectively evaluate (using information from the anomalies preceding the **M** 7.3 event) the conditional probability of each anomaly leading to a large earthquake of **M** ≥ 7.0.

### (S) Secular Probability Forecast

First, we need to evaluate the unconditional secular probability of an earthquake of **M** ≥ 7 in the rectangular target region (K-Region) around the **M** 6.5 earthquake epicenter bounded by dashed lines in Figure 1b. There were 182 earthquakes in the JMA hypocenter catalog of **M** ≥ 4 in the K-Region from 1923 to March 2016, and the *b*-value estimate of the magnitude–frequency is 0.99. Thus, the probability of an **M** ≥ 7 earthquake in this region is $0.5821 \times 10^{-5}$ events per day, assuming the Gutenberg–Richter law of magnitude–frequency. Alternatively, I applied the epidemic-type aftershock sequence (ETAS) model (Ogata, 1988) to the same data, and obtained its maximum-likelihood estimates. Thus, the background seismicity

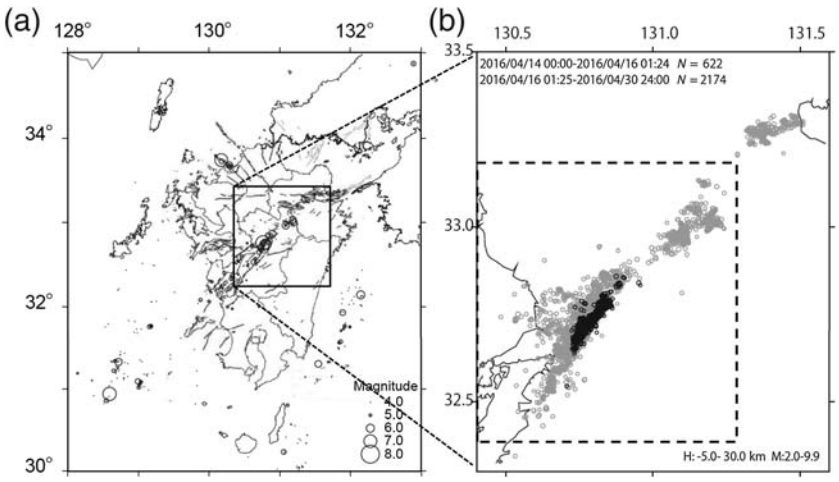


▲ **Figure 1.** (a) Shallow earthquakes of **M** ≥4 (circles) down to 30 km depth in the period 2000–2016 in and around Kyushu superimposed on active fault segments map. (b) Aftershocks (**M** ≥2, gray circles) of the **M** 7.3 Kumamoto earthquake and aftershocks (**M** ≥2, black circles) of the **M** 6.5 event before the **M** 7.3 earthquake. The rectangular area bounded by dashed lines (K-Region) is set to evaluate the secular probabilities of a possible **M** ≥7 earthquake (see the Secular Probability Forecast section for the detail).

rate ($\mu$-value) of the ETAS model together with the $b$-value leads to an alternative secular probability of $0.2427 \times 10^{-5}$ events per day for an **M** ≥7 earthquake in this region.

### (A) Long-Term Forecast

The Earthquake Research Committee (ERC, 2015) of Japan has evaluated long-term probabilities of 30-yr active fault rupture incidences of **M** ≥6.8, targeting forecasts of earthquakes of **M** ≥7 in inland Japan. The ERC estimated the probability in elapsed time since the last rupture using the Brownian passage time (BPT) distribution (Matthews *et al.*, 2002), estimating the cumulative stress rate from recurrence intervals and geological information. On the other hand, the aperiodicity coefficient ($\alpha$-value) of the BPT model is set to the same value throughout inland Japan. Thus, the ERC evaluated a 0.9% probability over 30 yrs for an **M** ≥7.0 rupture on the Futagawa fault, which is the proximate fault from the **M** 6.5 earthquake on the Hinagu fault.

The ERC also divided Kyushu Island into three regions, taking into account the combinations of multiple active faults. For each region, the ERC simulated the BPT for each fault, taking account of the uncertainty of the last occurrence. Thus, the probability of ruptures on one of the active faults in central Kyushu ranged 18%–27% (95% range) for 30 yrs with 21% as the median value. In addition, I tentatively assigned 10.5%, a half probability for central Kyushu, for the K-Region indicated in Figure 1b, which is about half the size of the central Kyushu region defined by the ERC.

Here, I discriminate (S) and (A) in the following way. I assume that the secular probability of an **M** 7 earthquake is a stationary Poisson process with a constant extremely small but nonzero occurrence rate. On the other hand, ruptures of an active fault assume a renewal process, and the rate increases from zero probability since the last **M** 7 class earthquake.

### (B) Medium-Term Forecast

I want to assign the medium-term conditional probability that major earthquakes before the **M** 6.5 earthquakes in Kyushu will trigger a similar or larger size earthquake in K-Region (see Fig. 1). Any earthquake can potentially trigger larger earthquakes. Figure 3 shows such an empirical relationship: the occurrence rate in a neighboring area per unit area is substantially higher than the rate in remote areas due to the triggering effects of large earthquakes. From this, the conditional probability an **M** ≥7 event inducing a proximate large earthquake within about 100–300 km is about 0.2%–0.5% per year.

Another conditional probability, that quiescence of previous aftershock activities in Kyushu Island relative to the ETAS model prediction will enhance inducement of a large earthquake in the K-Region, is available. Actually, the aftershock activity of the first **M** 6.5 earthquake was significantly lower relative to the ETAS model after the largest aftershock (**M** 6.4). Moreover, the aftershock sequences of the 2005 **M** 7.0 Fukuoka-Ken-Oki and 2016 Western Satsuma-Oki earthquakes in Kyushu indicate the relative quiescence (Kumazawa, Ogata, and Tsuruoka, 2016). Physical interpretations of these quiescence phenomena in this particular case have not yet been known until now. There may be various possible reasons for the relative quiescence of aftershock activities, but some are known to be caused by the stress shadow covering the aftershock zone, which is due to the precursory slow slip on neighboring faults (see Ogata, 2006, 2007, 2010, 2011b).

In this regard, Ogata (2001) studied the probability gain of the relative quiescence using diagnostic analysis, fitting the ETAS model to their seismicity data. Out of 76 analyzed aftershock sequences from 1925 to 1999 in Japan, 34 aftershock sequences have a significant changepoint followed by quiescence relative to the ETAS prediction. Figure 4a–c indicates triggering effects, showing again that probability gains depend on distance from the mainshock. Furthermore, the broken line connecting the sign Q in Figure 4c shows that the probability gain in the neighboring region is about 10 times higher than in remote areas in the case of relative quiescence in contrast to normal activity. Specifically, the conditional probability of inducing an **M** 7 class large earthquake (within an ~100 or 300 km radius and within 6 yrs) is about 1% or 2% per year, respectively. Hence, I assigned these probabilities in the K-Region (see Table 2).

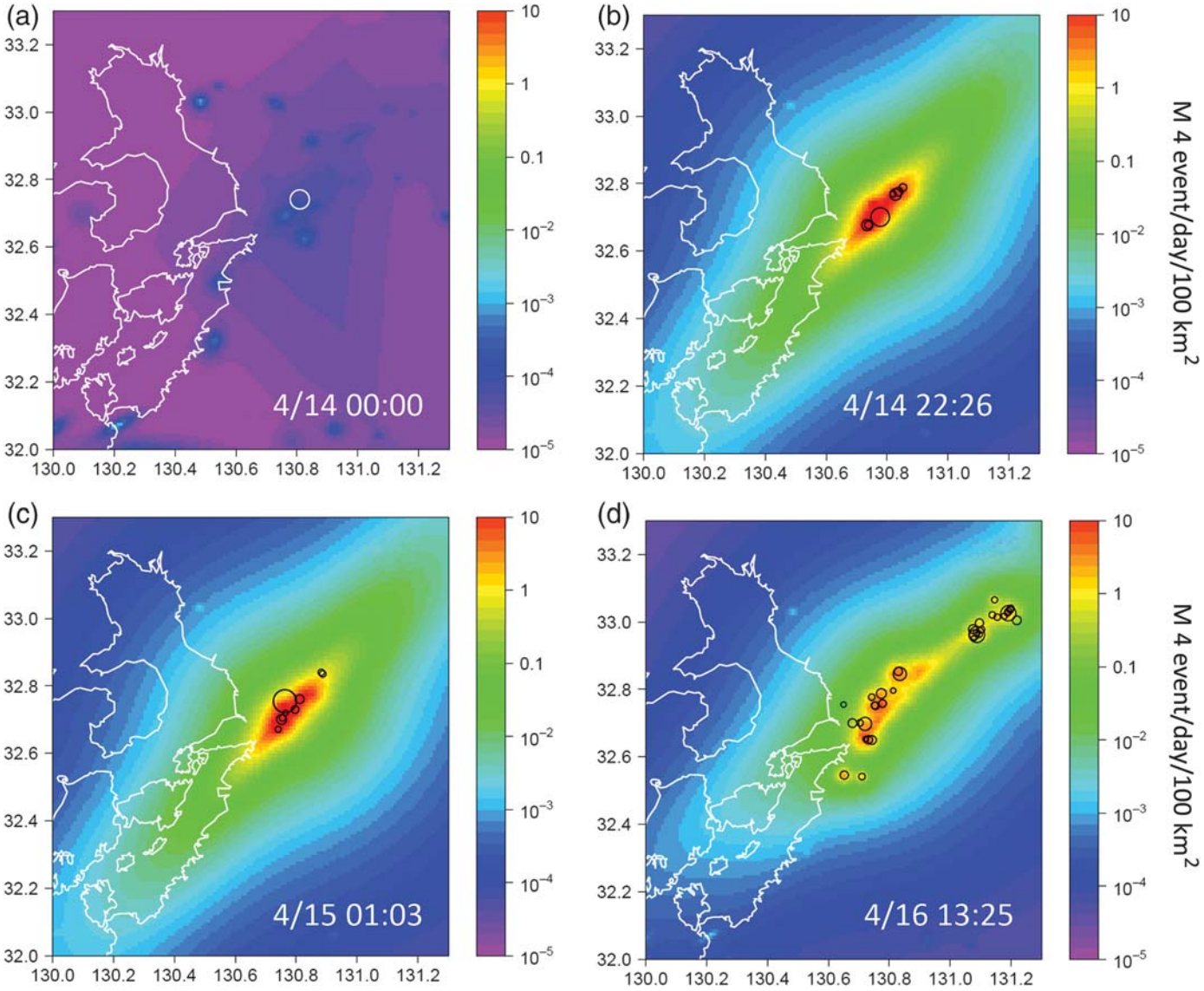


▲ **Figure 2.** Snapshots of probability forecasts of **M** ≥4 earthquakes at the indicated date and time in each panel, before and after the 2016 Kumamoto earthquake, obtained using the hierarchical space–time epidemic-type aftershock sequence (HIST-ETAS) model. The circles indicate actual **M** ≥4 earthquakes occurring during the forecast periods. Each forecast period lasts until the occurrence of (a) the **M** 6.5 earthquake, (b) the **M** 6.4 earthquake, and (c) the **M** 7.3 earthquake, respectively. The circles in (d) are from a 24-hr span starting 12 hrs after the **M** 7.3 earthquake. Color scale of the image shows expected number of **M** ≥4 earthquakes per 100 km$^2$ per day.

### (C) Short-Term Forecast

First, I automatically grouped ongoing earthquake clusters throughout Japan in real time using the single-link clustering (Frohlich and Davis, 1990) method. This link criterion was determined to roughly match the set of clusters obtained by a magnitude-based clustering algorithm, where the mainshock magnitude determines the size of the space–time window, except that it includes a 30-day time span before the mainshock (Ogata *et al.*, 1995, 1996). Then, I discriminated a cluster as a foreshock–mainshock type if the largest earthquake within the cluster from the beginning is replaced by a larger earthquake with a magnitude difference of 0.45 or more.

The first **M** 6.5 earthquake in K-Region takes a foreshock probability $p_0$ of about 2% per month (regional foreshock probability) for a mainshock of **M** 7.0 or larger. Then, for subsequent earthquakes, I forecast the foreshock probability $p_c$ of the cluster $c$ until the current time. This probability consists of variables of time intervals, distances, and magnitude increments between all earthquakes before the current time in cluster $c$. See Ogata *et al.* (1996) for details of the model and Ogata and Katsura (2012) for the forecast demonstration.

I evaluated, retrospectively, the probability of having an **M** ≥7.0 earthquake during a 30-day period following an **M** 6.5 earthquake. I calculated $p_c$ at the occurrence time of each subsequent earthquake using the logit model (equation A5). Thus, as shown in shaded period of Figure 5, the foreshock probability increased from $p_0 \approx 2\%$ (regional

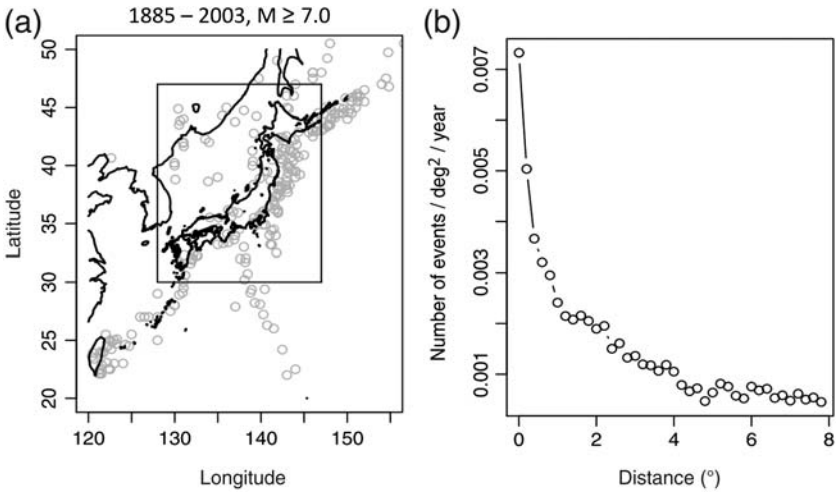


▲ **Figure 3.** Triggering effects. (a) Epicenter locations of **M** ≥7 earthquakes in and around Japan between 1885 and 2003, obtained using the Utsu catalog (Utsu, 1979b, 1982) and the Japan Meteorological Agency (JMA) catalog. (b) Histogram of distances between **M** ≥7 earthquakes in the inner rectangular region and those that occurred later in the entire region.

foreshock probability) to $p_c$ of around 5% per month, and it drastically decreased after the **M** 7.3 earthquake.

### Multielements Probabilities in K-Region

Table 2 summarizes the conditional probabilities after transforming each probability of anomaly events A, B, and C mentioned above to the probability per day. Assuming independence between the events A, B, and C in different time scales, Table 3 provides the predicted probabilities calculated based on the multielements probability formula (equation A1). Namely, the probability lists in Table 3 depend on selected combinations of assessed probabilities within A, B, and C in Table 2 and the evaluation of the probability of **M** ≥7.0 earthquake occurrence in K-Region, which varies 0.2%–20% per day, 0.5%–40% per three days, 1%–60% per week, and 5%–90% per month.

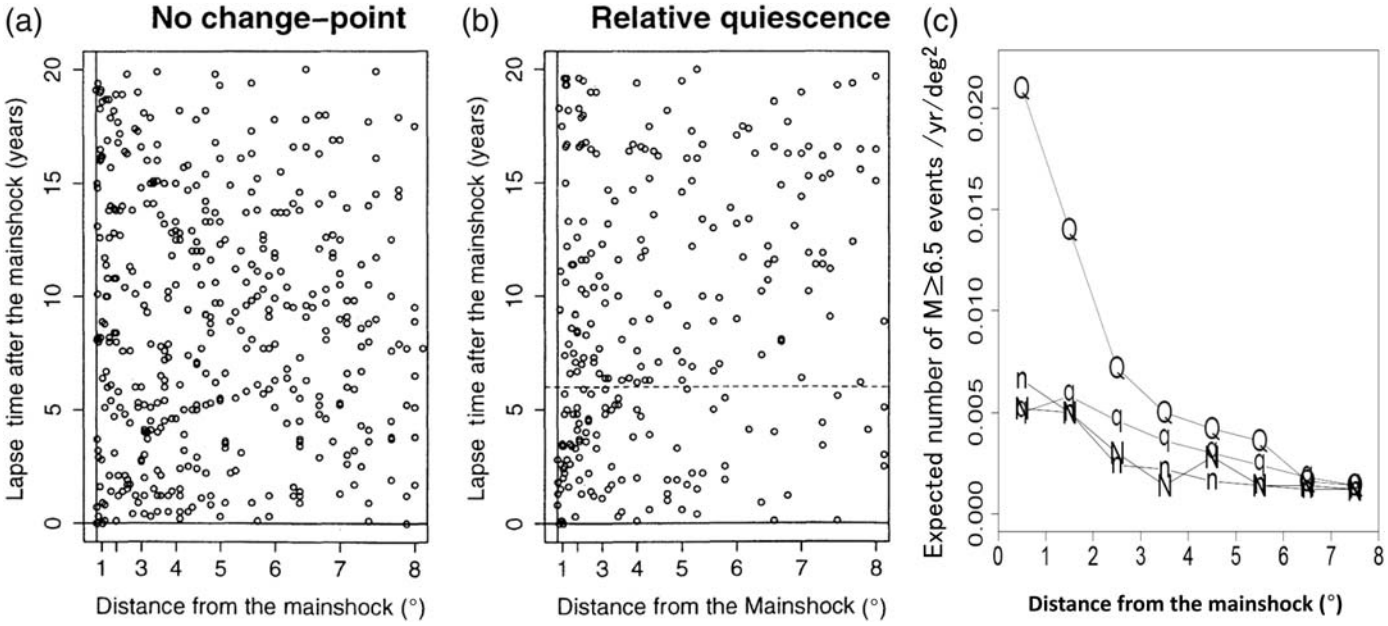


▲ **Figure 4.** Discriminated patterns of the occurrences of large earthquakes. (a,b) Superposed plots of time difference versus spatial distance to future **M** ≥6.5 earthquakes from the mainshock of the investigated aftershocks; where (a) shows superposition for 43 mainshocks whose aftershock sequences have no change point and (b) shows superposition of 34 mainshocks whose aftershock sequences show relative quiescence. The abscissa of (a) and (b) is scaled by the square of the distance to be proportional to the area of the disk with the given distance as radius. The concentration of mainshocks in distance during the first 6 yrs is notably stronger than those of the other 14 yrs in (b), and those throughout the 20 yrs in (a). (c) Average numbers of subsequent large earthquakes (**M** ≥6.5) per unit area (1 square degree) against distance in degrees from the **M** ≥6.5 mainshock of the investigated aftershock sequence. The broken lines with upper case Q and N represent the case during the period of first 6 yrs where aftershock activity became quiet and where aftershock activity was normal relative to the ETAS model, respectively. The lines with lowercase q and n represent the case during the period from 7 to 20 yrs where aftershock activity became quiet or where activity was normal relative to the ETAS, respectively. See Ogata (2001) for the estimation procedure.

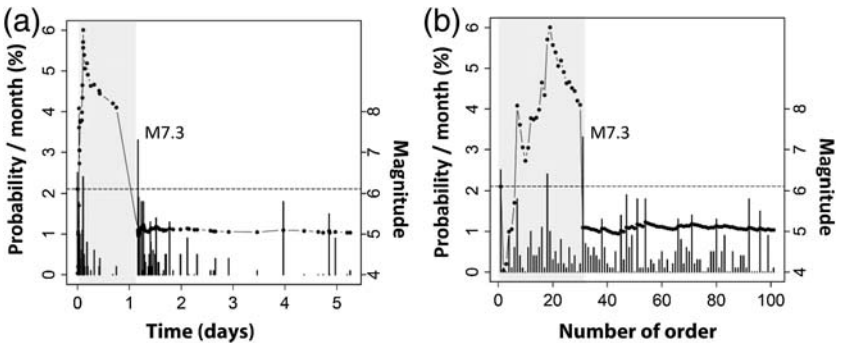


▲ **Figure 5.** Foreshock probabilities $p_c$ plotted against (a) ordinary time and (b) sequential order at each time of **M** ≥4 earthquakes before and after the **M** 7.3 earthquake.

Furthermore, I evaluated the probability for the period before the occurrence of foreshocks. During that period, there were two **M** 7 earthquakes in Kyushu Island in 2005 and 2017 (Fig. 1a). The distances from each epicenter to the K-Region are about 1° and 3°, respectively. Thus, from the empirical relationship in Figure 3, I can expect an **M** ≥7 event in the K-Region to happen about 0.002–0.005 times per year for the triggering effect. I then recognized the relative quiescence after some time in the latter part of the **M** 7 aftershocks, which is given to be about 0.01–0.02 times per year. The relative quiescence shows ∼3–4 times enhancement factor for the triggering effect at about 100–300 km distance as shown in Figure 4. This evaluation for such periods with corresponding multielement probabilities is given in Table 4. Comparing Table 3 with Table 4, we can see how substantially the foreshock forecast enhances the joint probability of **M** ≥7 event.

## DISCUSSIONS AND CONCLUSIONS

We assessed the probability value for each item after accumulation of observation data over many years. In this article, I calculated the conditional probabilities using accumulated seismicity data. Earthquake occurrence data are the largest amount recorded in any region for the longest period of time among various geophysical data, although there are differences in detection capability. First, I used the active faults data compiled by the ERC of Japan to assess the long-term probabilities. Second, I used the JMA and Utsu's hypocenter catalog (Utsu, 1979b, 1982), which ranges 120 yrs, to assess the triggering effects of large earthquakes. Third, I used the JMA hypocenter catalog and aftershock occurrence times from the former JMA document, ranging 70 yrs, for empirical results against the studies of 76 aftershock sequences. Finally, I identified a foreshock probability forecasting procedure using 50 yrs of JMA data and tested the performance of foreshock forecasts over an additional 17 yrs.

However, except for seismicity anomalies, it has been difficult to gather cases of earthquake prediction in other monitoring fields within a short time. Still, I wish to use data on various types of anomalies, such as locally intensive monitoring in the Izu area at a given time, to evaluate the probability gain of causing large earthquakes. The following discusses some issues on the outlook using a similar and extended approach in seismicity and other monitoring fields.

### Alarm Rate Issues

Utsu (1977) called the probability of the perceived abnormality of a certain earthquake prediction the earthquake's alarm rate. However, so far, the alarm rate has been very low. Namely, we observed very few clear precursory phenomena preceding major earthquakes, which in fact prevented me from stably assessing probability gains. Therefore, we had very little occasion to forecast using the multielements formula.

**Table 2**
**Conditional Probability Assessments for an M ≥7 Earthquake in the K-Region**

| Unit Time | Seismicity Indicators and Anomalies | 30 yrs | 1 yr | 1 month | 1 day |
|---|---|---|---|---|---|
| Secular | | | | | |
| $S_1$ | ETAS-$\mu$ and G–R law | | | | 0.000002747 |
| $S_2$ | #(**M** ≥4) and G–R law | | | | 0.000005821 |
| Long Term | | | | | |
| $A_1$ | Futagawa fault | 0.009 | 0.0003 | | 0.00000082 |
| $A_2$ | K-Region | 0.105 | 0.0035 | | 0.00000958 |
| $A_3$ | Central Kyushu | 0.210 | 0.007 | | 0.00001917 |
| Medium Term | | | | | |
| $B_1$ | Triggering | | 0.005 | | 0.00001369 |
| $B_2$ | Quiescence | | 0.02 | | 0.00005476 |
| Short Term | | | | | |
| C | Foreshocks | | | 0.05 | 0.00166667 |

Assessment of the secular probabilities and conditional probabilities of an **M** ≥7 earthquake based on information for each prediction interval are listed. #(**M** ≥4), Number of **M** ≥4 earthquakes in 1926 to March 2016; ETAS, epidemic-type aftershock sequence; G–R, Gutenberg–Richter.

**Table 3**
**Multielement Prediction of an M ≥7 Earthquake in the K-Region**

| Unit Time | 1 day | 3 days | 1 week | 1 month |
|---|---|---|---|---|
| $P(S_1\|A_1\cap B_2\cap C)$ | 0.0099 | 0.029 | 0.066 | 0.24 |
| $P(S_1\|A_2\cap B_2\cap C)$ | 0.10 | 0.26 | 0.45 | 0.79 |
| $P(S_1\|A_3\cap B_2\cap C)$ | 0.19 | 0.41 | 0.62 | 0.88 |
| $P(S_2\|A_1\cap B_2\cap C)$ | 0.0017 | 0.0051 | 0.012 | 0.051 |
| $P(S_2\|A_2\cap B_2\cap C)$ | 0.020 | 0.057 | 0.12 | 0.39 |
| $P(S_2\|A_3\cap B_2\cap C)$ | 0.039 | 0.11 | 0.22 | 0.56 |

The probability of an **M** ≥7 earthquake, conditional on the information available for joint prediction intervals. Each letter with or without subscript corresponds to those in Table 2.

**Table 4**
**Multielement Prediction of an M ≥7 Earthquake in the K-Region without Foreshocks**

| Unit Time | 1 month | 6 months | 1 yr | 3 yrs |
|---|---|---|---|---|
| $P(S_1\|A_2\cap B_1)$ | 0.00068 | 0.0041 | 0.0082 | 0.025 |
| $P(S_1\|A_2\cap B_2)$ | 0.0027 | 0.016 | 0.033 | 0.095 |
| $P(S_2\|A_2\cap B_1)$ | 0.0013 | 0.0080 | 0.016 | 0.047 |
| $P(S_2\|A_2\cap B_2)$ | 0.0053 | 0.031 | 0.062 | 0.17 |

The probability of an **M** ≥7 earthquake in the K-Region before the **M** 6.5 foreshock sequence, conditional on the information available for joint prediction intervals. Each letter with or without subscript corresponds to those in Table 2.

To improve the low alarm rate, we need to aim for sensitive detection of anomalies by statistical diagnostic analysis of observed data. Namely, when records fluctuate over time, we need to seek and define the anomaly not only by a simple criterion when the time records exceed a certain level but also by discovering structural changes in the records. For this, we should establish a standard reference model that predicts data in an ordinary state. Then, we search for misfits of the data relative to the predicted values. Indeed, there are subtle misfits that we can discover after a diagnostic analysis of seismicity using the ETAS model as discussed in the Medium-Term Forecast section. After identifying abnormalities, many efforts to quantify the statistical causalities and evaluate the probability gain are required even if the hitting ratios of target earthquakes by respective anomalies are low.

In addition, the statistical discrimination of a precursory slip from slow slips in general is necessary for medium-term or short-term conditional probability assessments. There are many frequent postseismic slips accompanying large earthquakes, swarms, and small repeating earthquakes on plate boundary interfaces (e.g., Nomura and Ogata, 2016). The probability gain of a respective slip must be statistically evaluated, although there will be regional differences among them. We have to study such statistical causality relative to neighboring large earthquakes.

Geodetic databases compiled from Global Positioning System (GPS) signals also account for a large portion of data recorded at dense stations in inland Japan since 1994 (Geographical Survey Institute [GSI], 2010). Geodetic anomalies would also be searched for in time series of baseline distances between GPS stations (e.g., Ogata, 2007, 2010, 2011b; Kumazawa *et al.*, 2010), in various strain time series within triangular regions of GPS stations, or in volumetric strain records (Kumazawa, Ogata, Kimura, *et al.*, 2016).

At the moment there is considerable difficulty in separating small slip signals (especially inland slips) from GPS location records in their operational monitoring despite the dense arrangement of GPS observation stations in inland Japan area. This is because earthquakes occur so frequently and records include not only GPS measurement errors but also the numerous coseismic and postseismic displacements of the small and medium earthquakes in surrounding areas. Indeed, the records seem to fluctuate dramatically, mixing various slow slips and fast slips, compared to the steady GPS records around Alice Springs, Australia (Wang and Bebbington, 2013). This fact encourages us to develop proper standard space–time geodetic models for separating signals. Thus, there is substantial room for developing statistical models and analytical methods for discriminating abnormal events.

For example, some statistical outliers in records of baseline distances between GPS stations may possibly relate to occurrences of strong earthquakes in some regions. Specifically, Wang *et al.* (2013) defined outliers related to the maximum fluctuation range of baseline expansion and contraction within a 10-day window and warned of medium-scale earthquakes in the surrounding area for a certain period of time with these abnormalities. They tested whether actual earthquakes occurred during the warning period using Molchan's error diagram (Molchan, 1991). Here, I would like to encourage a search for a causal relationship between series of anomalies and series of strong earthquakes in a target region and an evaluation of probability gain (Ogata and Akaike, 1982; Ogata *et al.*, 1982; Kumazawa, Ogata, Kimura, *et al.*, 2016). In addition to geodetic records, it is necessary to maintain a record of clearly defined abnormal events including those involving magnetic or electric fields (Zhuang *et al.*, 2005, 2014; Han *et al.* 2016).

We need to statistically distinguish whether such abnormal phenomena can be predictive of a large earthquake, analyze their statistical causal relations to the occurrence of a strong earthquake, and link the change of the degree of risk or urgency to stochastic prediction. Ogata (2013, 2017) reviewed such models and methods for earthquake predictability studies.

## Independence Assumptions and Multiplicative Models

Utsu (1977, 1982) derived a multielements prediction formula (equation A1) that assumes that each of the anomalies appearing in nonoverlapping periods are independent from each other, given a target of a large earthquake. Thus, long-term, medium-term, and short-term anomalies are nearly indepen-

dent when ignoring very short common time intervals relative to the longer-term period.

We can assess the probability value for each item after accumulating observation data over many years, but it is difficult to gather many cases of earthquake prediction within a short time. Hence, rigorous testing of the independence hypothesis is not easy unless we have enough experiments, especially when including enough long-term anomalies. Therefore, at worst, we should regard the joint probability values obtained in Tables 1 and 2 as reference values indicating the upper limit.

Anomalies appearing within a similar period may be well correlated to each other, so we first consider the general form as given in equation (A4), taking account of the correlations. For example, Ogata *et al.* (1996) considered the $\varphi$ function in equation (A4) a logistic regression for the foreshock probability in terms of the multinominal polynomial expansion, taking into account the dependency between variables of time differences, epicenter separations, and magnitude increments within the same earthquake cluster. In this case, using the Akaike information criterion (AIC; Akaike, 1974), the linear relation of the form (equation A5) was selected, which supports the independence hypothesis between variables as represented by equation (A5).

On the other hand, even if some dependency may exist among useful variables for predictions, the conditional intensity function with multiplicative form, as given in equation (A7), can often provide better prediction performance than using only one variable. Rhoades *et al.* (2014, 2016) and Shebalin *et al.* (2014) modeled this in such a way to take long-term, medium-term, and short-term information into consideration. Performance of these models were tested by the Molchan diagram (Molchan, 1991) and likelihood-ratio statistics. We can search optimal multiplicative models for prediction using the AIC. For example, an additive model with clustering effect (ETAS) in the particular aftershock activity and earth-tide records was improved by a similar multiplicative model (Iwata and Katao, 2006a,b; Iwata, 2012).

## DATA AND RESOURCES

The Japan Meteorological Agency (JMA) unified hypocenter catalog after 1923 is available at the JMA website (http://www.data.jma.go.jp/svd/eqev/data/bulletin/hypo_e.html, last accessed October 2016). Some sequences of felt/unfelt aftershocks before 1926 are obtained by some JMA observatories recorded in the *Kishoyoran* (the *Geophysical Review of the JMA*, and the *Zisin Geppou* (the *Seismological Bulletin of the JMA*). We also used the Utsu catalog for the period 1885–1980 (Utsu, 1979b, 1982). ◼

## ACKNOWLEDGMENTS

The author would like to thank Zhigang Peng and anonymous referees for their comments on clarification of the article. Thanks also to the Japan Meteorological Agency (JMA), the National Research Institute for Earth Science and Disaster Resilience (NIED), and universities for providing the data. This article is partly supported by the KAKENHI Grant of Japan Society for the Promotion Science, Number 17H00727.

## REFERENCES

Akaike, H. (1974). A new look at the statistical model identification, *IEEE Trans. Automat. Contr.* **19,** no. 6, 716–723.

Akaike, H. (1985). Prediction and entropy, in *A Celebration of Statistics, The ISI Centenary Volume*, A. C. Atkinson and S. E. Fienberg (Editors), Springer-Verlag, New York, New York, 1–24.

Aki, K. (1981). A probabilistic synthesis of precursory phenomena, in *Earthquake Prediction*, D. W. Simpson and P. G. Richards (Editors), Maurice Ewing Series, Vol. 4, American Geophysical Union, Washington, D.C., 566–574.

Cao, T., and K. Aki (1983). Assigning probability gain for precursors of four large Chinese earthquakes, *J. Geophys. Res.* **88,** no. B3, 2185–2190.

Coordinating Committee of Earthquake Prediction (CCEP) (1976–1978). *Report of the Coordinating Committee of Earthquake Prediction 16-20*, available at http://cais.gsi.go.jp/YOCHIREN/report.html (last accessed May 2017).

Cox, D. R., and E. J. Snell (1989). *Analysis of Binary Data*, Second Ed., Chapman & Hall/CRC, London, United Kingdom.

Earthquake Research Committee (ERC) (2015). *Long Term Evaluation of Active Faults in Kyushu Area*, First Ed., available at http://www.jishin.go.jp/main/chousa/13feb_chi_kyushu/kyushu_point.pdf (last accessed May 2017) (in Japanese).

Frohlich, C., and S. D. Davis (1990). Single-link cluster analysis as a method to evaluate spatial and temporal properties of earthquake catalogs, *Geophys. J. Int.* **100,** no. 1, 19–32.

Geographical Survey Institute (GSI) (2010). *Long-Term Information on Crustal Movement Detected by GNSS-Based Control Point*, available at http://mekira.gsi.go.jp/project/f3_10_5/en/index.html (last accessed May 2017).

Han, P., K. Hattori, J. Zhuang, C-H. Chen, J-Y. Liu, and S. Yoshida (2016). Evaluation of ULF seismo-magnetic phenomena in Kakioka, Japan by using Molchan's error diagram, *Geophys. J. Int.* **208,** 482–490.

Hashimoto, M., M. Savage, T. Nishimura, H. Horikawa, and H. Tsutsumi (Editors) (2016–2017). 2016 Kumamoto earthquake sequence and its impact on earthquake science and hazard assessment, special issue, *Earth Planets Space* **69**, available at https://www.springeropen.com/collections/keq (last accessed May 2017).

Iwata, T. (2012). Earthquake triggering caused by the external oscillation of stress/strain changes, *CORSSA* 1–27, doi: 10.5078/corssa-65828518.

Iwata, T., and H. Katao (2006a). Correlation between the phase of the moon and the occurrences of microearthquakes in the Tamba region through point-process modeling, *Geophys. Res. Lett.* **33,** L07302, doi: 10.1029/2005GL025510.

Iwata, T., and H. Katao (2006b). Correlation between the phase of the moon and the occurrences of microearthquakes in the Tamba region by a modified conditional intensity model, presented at the *Annual Meeting of Seismological Society of Japan*, Nagoya International Convention Center, 31 October–2 November 2006, 212 pp.

Japan Meteorological Agency (JMA) (2016). *Prediction and Information Services for the Tokai Earthquake*, available at http://www.jma.go.jp/jma/en/Activities/earthquake.html (last accessed May 2017).

Kumazawa, T., Y. Ogata, and S. Toda (2010). Precursory seismic anomalies and transient crustal deformation prior to the 2008 $M_w$ 6.9 Iwate-Miyagi Nairiku, Japan, earthquake, *J. Geophys. Res.* **115,** no. B10312, doi: 10.1029/2010JB007567.

Kumazawa, T., Y. Ogata, K. Kimura, K. Maeda, and A. Kobayashi (2016). Background rates of swarm earthquakes that are synchronized with volumetric strain changes, *Earth Planet. Sci. Lett.* **442,** 51–60, doi: 10.1016/j.epsl.2016.02.049.

Kumazawa, T., Y. Ogata, and H. Tsuruoka (2016). Statistical monitoring of seismicity in Kyushu District before the occurrence of the 2016 Kumamoto earthquakes of M 6.5 and M 7.3, *Report of the Coordinating Committee for Earthquake Prediction*, Vol. 96, 642–651, available at http://cais.gsi.go.jp/YOCHIREN/report/kaihou96/12_21.pdf (last accessed May 2017).
Maeda, K., and A. Yoshida (1990). A probabilistic estimation of earthquake occurrence on the basis of the appearance times of multiple precursory phenomena, *J. Phys. Earth* **38,** no. 6, 431–444.
Matthews, M. V., W. L. Ellsworth, and P. A. Reasenberg (2002). A Brownian model for recurrent earthquakes, *Bull. Seismol. Soc. Am.* **92,** no. 6, 2233–2250.
Molchan, G. M. (1991). Structure of optimal strategies of earthquake prediction, *Tectonophysics* **193,** no. 4, 267–276.
Nanjo, K. Z., H. Tsuruoka, N. Hirata, and T. H. Jordan (2011). Overview of the first earthquake forecast testing experiment in Japan, *Earth Planets Space* **63,** no. 3, 159–169.
Nomura, S., and Y. Ogata (2016). Foreshock forecast probabilities of the M 7.3 Kumamoto earthquake of 2016, *Report of the Coordinating Committee for Earthquake Prediction*, Vol. 96, 642–651, available at http://cais.gsi.go.jp/YOCHIREN/report/kaihou96/12_22.pdf (last accessed May 2017).
Ogata, Y. (1988). Statistical models for earthquake occurrences and residual analysis for point processes, *J. Am. Stat. Assoc.* **83,** no. 401, 9–27.
Ogata, Y. (2001). Increased probability of large earthquakes near aftershock regions with relative quiescence, *J. Geophys. Res.* **106,** no. B5, 8729–8744.
Ogata, Y. (2006). Monitoring of anomaly in the aftershock sequence of the 2005 earthquake of M 7.0 off coast of the western Fukuoka, Japan, by the ETAS model, *Geophys. Res. Lett.* **33,** L01303, doi: 10.1029/2005GL024405.
Ogata, Y. (2007). Seismicity and geodetic anomalies in a wide area preceding the Niigata-Ken-Chuetsu earthquake of 23 October 2004, central Japan, *J. Geophys. Res.* **112,** no. B10301, doi: 10.1029/2006JB004697.
Ogata, Y. (2010). Anomalies of seismic activity and transient crustal deformations preceding the 2005 M 7.0 earthquake west of Fukuoka, *Pure Appl. Geophys.* **167,** nos. 8/9, 1115–1127, doi: 10.1007/s00024-010-0096-y.
Ogata, Y. (2011a). Significant improvements of the space–time ETAS model for forecasting of accurate baseline seismicity, *Earth Planets Space* **63,** no. 3, 217–229, doi: 10.5047/eps.2010.09.001.
Ogata, Y. (2011b). Pre-seismic anomalies in seismicity and crustal deformation: Case studies of the 2007 Noto Hanto earthquake of M 6.9 and the 2007 Chuetsu-Oki earthquake of M 6.8 after the 2004 Chuetsu earthquake of M 6.8, *Geophys. J. Int.* **186,** no. 1, 331–348, doi: 10.1111/j.1365-246X.2011.05033.x.
Ogata, Y. (2013). A prospect of earthquake prediction research, *Stat. Sci.* **28,** no. 4, 521–541, doi: 10.1214/13-STS439.
Ogata, Y. (2017). Statistics of earthquake activity, *Annu. Rev. Earth Planet. Sci.* **45,** no. 1, doi: 10.1146/annurev-earth-063016-015918.
Ogata, Y., and H. Akaike (1982). On linear intensity models for mixed doubly stochastic Poisson and self-exciting point processes, *J. Roy. Stat. Soc. B* **44,** no. 1, 102–107.
Ogata, Y., and K. Katsura (2012). Prospective foreshock forecast experiment during the last 17 years, *Geophys. J. Int.* **191,** no. 3, 1237–1244, doi: 10.1111/j.1365-246X.2012.05645.x.
Ogata, Y., H. Akaike, and K. Katsura (1982). The application of linear intensity models to the investigation of causal relations between a point process and another stochastic process, *Ann. Inst. Stat. Math.* **34,** no. 2, 373–387.
Ogata, Y., T. Utsu, and K. Katsura (1995). Statistical features of foreshocks in comparison with other earthquake clusters, *Geophys. J. Int.* **121,** 233–254.
Ogata, Y., T. Utsu, and K. Katsura (1996). Statistical discrimination of foreshocks from other earthquake clusters, *Geophys. J. Int.* **127,** no. 1, 17–30.
Rhoades, D. A., A. Christophersen, and M. C. Gerstenberger (2016). Multiplicative earthquake likelihood models based on fault and earthquake data, *Bull. Seismol. Soc. Am.* **105,** no. 6, doi: 10.1785/0120150080.
Rhoades, D. A., M. C. Gerstenberger, A. Christophersen, J. D. Zechar, D. Schorlemmer, M. J. Werner, and T. H. Jordan (2014). Regional earthquake likelihood models II: Information gains of multiplicative hybrids, *Bull. Seismol. Soc. Am.* **104,** no. 6, 3072–3083, doi: 10.1785/0120140035.
Shebalin, P. N., C. Narteau, J. D. Zechar, and M. Holschneider (2014). Combining earthquake forecasts using differential probability gains, *Earth Planets Space* **66,** no. 37, 1–14, doi: 10.1186/1880-5981-66-37.
Utsu, T. (1977). Probability in earthquake prediction, *Zisin* **30,** 179–185.
Utsu, T. (1979a). Calculation of the probability of success of an earthquake prediction (In the case of Izu-Oshima-Kinkai earthquake of 1978), *Rep. Coord. Comm. Earthq. Predict.* **21,** 164–166, available at http://cais.gsi.go.jp/YOCHIREN/report/kaihou21/07_04.pdf (last accessed May 2017).
Utsu, T. (1979b). Seismicity of Japan from 1885 through 1925: A new catalog of earthquakes of M ≥ 6 felt in Japan and smaller earthquakes which caused damage in Japan, *Bull. Earthq. Res. Inst.* **54,** 254–308 (in Japanese).
Utsu, T. (1982). Catalog of large earthquakes in the region of Japan from 1885 through 1980, *Bull. Earthq. Res. Inst.* **57,** 401–463.
Vere-Jones, D. (1978). Earthquake prediction—A statistician's view *J. Phys. Earth* **26,** 129–146.
Wang, T., and M. Bebbington (2013). Identifying anomalous signals in GPS data using HMMs: An increased likelihood of earthquakes? *Comput. Stat. Data Anal.* **58,** 27–44.
Wang, T., J. Zhuang, T. Kato, and M. Bebbington (2013). Assessing the potential improvement in short-term earthquake forecasts from incorporation of GPS data, *Geophys. Res. Lett.* **40,** 2631–2635.
Zhuang, J., and C. Jiang (2012). Scoring annual earthquake predictions in China, *Tectonophysics* **524/525,** 155–164, doi: 10.1016/j.tecto.2011.12.033.
Zhuang, J., Y. Ogata, D. Vere-Jones, L. Ma, and H. Guan (2014). Statistical modeling of earthquake occurrences based on external geophysical observations: With an illustrative application to the ultra-low frequency ground electric signals observed in the Beijing region, in *Seismic Imaging, Fault Rock Damage and Healing*, Y. Li (Editor), De Gruyter/Higher Education Press, Berlin, Germany/Beijing, China, 351–376.
Zhuang, J., D. Vere-Jones, H. Guan, Y. Ogata, and L. Ma (2005). Preliminary analysis of observations on the ultra-low frequency electric field in a region around Beijing, *Pure Appl. Geophys.* **162,** 1367–1396 (with data).

## APPENDIX

## MULTIELEMENTS PROBABILITY FORMULA AND ITS EXTENSIONS

Assuming that anomalies $\{A_n, n = 1, 2, \cdots, N\}$ are mutually independent, conditional on an impending earthquake $M$ of magnitude **M** or greater, in such a way that $P(\bigcap_{n=1}^{N} A_n|M) = \prod_{n=1}^{N} P(A_n|M)$ holds, Utsu (1977) derived the conditional probability of an earthquake of magnitude $M$ or greater occurring within a time interval $\Delta$

$$P\left(M|\bigcap_{n=1}^{N} A_n\right)=\left[1+\prod_{n=1}^{N}\{P(M|A_n)^{-1}-1\}/\{P(M)^{-1}-1\}^{N-1}\right]^{-1}, \tag{A1}$$

which is referred to as the multielements probability formula. Aki (1981) also derived the same formula using the Bayes rule and further approximated equation (A1) by

$$P\left(M|\bigcap_{n=1}^{N}A_n\right)\approx P(M)\prod_{n=1}^{N}\frac{P(M|A_n)}{P(M)} \tag{A2}$$

when the time interval $\Delta$ is small. Each probability ratio in the right side of equation (A2) is called the probability gain, which measures the efficiency of an anomaly as a precursor. The multielements prediction formula is derived based on a strong assumption of independency between anomalous events. Among anomalous long-term, medium-term, and short-term phenomena, we may well assume independency to each other.

When we have many kinds of anomalies, independency is not necessarily justified. In such a case, it is necessary to consider the generalized version. For a probability value $p$ $(0 \le p \le 1)$, consider the logit transformation

$$f = \text{logit}\,p, \quad \text{in which } p = 1/(1+e^{-f}) \tag{A3}$$

(e.g., Cox and Snell, 1989), and consider nonlinear logistic regression

$$\text{logit}P\left(M|\bigcap_{n=1}^{N}A_n\right)=\varphi(f_1,f_2,...,f_N;f_0), \tag{A4}$$

in terms of $f_n = \text{logit}P(M|A_n)$ for $n = 1, 2, ..., N$ and $f_0 = \text{logit}P(M)$. The Utsu formula in equation (A1) is same as

$$\text{logit}P\left(M|\bigcap_{n=1}^{N}A_n\right)=\sum_{n=1}^{N}\text{logit}P(M|A_n)-(N-1)\text{logit}P(M), \tag{A5}$$

which means that the function $\varphi$ becomes linear with respect to the probability logits and supports the independence hypothesis between variables. Here, the Akaike information criterion (AIC; Akaike, 1974, 1985) is useful for selecting specific competing models of equation (A4) including equation (A5); see Ogata *et al.* (1996) for a comparison to derive the foreshock forecast formula. A model of the smaller AIC values is expected to be a better predictive model (Akaike, 1985).

For space–time evaluation of probability gains, a stochastic point process modeling is useful for predicting space–time stochastic intensity rates of expected earthquakes. For example, Maeda and Yoshida (1990) evaluate a time to failure after the observation of multiple independent long-term, medium-term, and short-term anomalies. This should enable us to calculate the probability of a large earthquake. If we consider conditional intensity function models

$$\lambda(t,x,y,M|H_t,F_t)\approx\frac{P\{\text{an event in}[t,t+\Delta t]\times[x,x+\Delta x]\times[y,y+\Delta y]\times[M,M+\Delta M]|H_t,F_t\}}{\Delta t\Delta x\Delta y\Delta M} \tag{A6}$$

that depend on occurrence history $\{H_t\}$ and data sets of various anomalies $F_t = \{F_t^k; k = 1, 2, ..., K\}$ that are mutually independent among $k$ conditional on their histories, then we can consider equation (A2) in such a way that

$$\lambda(t,x,y,M|H_t,F_t^1,...,F_t^K) = \lambda_0(t,x,y,M|H_t)\prod_{k=1}^{K}\frac{\lambda_k(t,x,y,M|H_t,F_t^k)}{\lambda_0(t,x,y,M|H_t)}, \tag{A7}$$

in which $\lambda_0(t,x,y,M|H_t)$ represents the conditional intensity for reference seismic activity. Vere-Jones (1978) referred to the ratios in equation (A7) as the risk enhancement factors. When a large earthquake is forecasted during a long period in some seismogenic region, one may use an approximated reference seismicity model such as stationary Poisson process $\lambda_0(M)$ (Utsu, 1979a) or nonhomogeneous spatial Poisson processes $\lambda_0(x,y,M)$ (Zhuang and Jiang, 2012).

Also, in general, the conditional intensity $\ln\lambda(t,x,y,M|H_t,F_t^1,...,F_t^N)$ represents a combination of $f_0 = \ln\lambda_0(t,x,y,M|H_t)$ and $f_n = \ln\lambda_n(t,x,y,M|H_t,F_t^n)$.

***Yosihiko Ogata***
***The Institute of Statistical Mathematics***
***10-3 Midori-Cho, Tachikawa***
***Tokyo 190-8562, Japan***
***ogata@ism.ac.jp***

Published Online 7 June 2017